DOI: 10.1002/ejic.200701322

Synthesis and Structural Characterization of a Tetrameric Ammonium Chloride Cluster

Nikola Schulenberg,[a] Olaf Hübner,[a] Elisabeth Kaifer,[a] and Hans-Jörg Himmel*[a]

Keywords: Atmospheric chemistry / Cluster compounds / Hydrogen bonding / Quantum chemical calculations

Herein we report the synthesis and structural characterization of a derivative of the molecular cluster $[NH_4Cl]_4$. The N and Cl atoms in this compound are located at alternating corners of a slightly distorted cube in the crystal phase and are bound together through N–H···Cl bridges. This structure is in good agreement with quantum chemical calculations carried out for the $[NH_4Cl]_4$ tetramer. ESI mass spectra recorded for the compound dissolved in different solvents indicate that the cluster is stable in relatively apolar solvents such as CH_2Cl_2.

Introduction

Nucleation is a key step in many laboratory and natural events and is, for example, important for the understanding of atmospheric processes such as the formation of troposphere aerosols.[1] Sulfate, nitrate, ammonium, sodium, and chloride account for 25–50% of the dry fine particle mass in the atmosphere.[2] NH_3 levels in the lower troposphere are above 10 ppt. The partial pressure of HCl in the planetary boundary layer, which originates for example from coal combustion and waste incineration, from sea-salt particles due to reaction of other acidic compounds with them, from volcanoes, and from the oxidation of methyl chloride in the atmosphere, frequently exceeds 1 ppb.[3] A knowledge of nucleation particle formation and their growth from these small molecules is therefore of great importance for the understanding of atmospheric chemistry. The formation of these particles is usually assumed to take place in the presence of water vapour, and there is still great debate as to whether or not formation of NH_4Cl particles in the gas phase could take place under dry conditions. The formation of NH_4Cl clusters from NH_3 and HCl in the gas phase has been studied in many theoretical and experimental works.[4,5] For example, $[(NH_4Cl)_nNH_4]^+$ ions have been detected by thermospray mass spectrometry.[6,7] Clusters with n = 3, 6, and 13 dominate the spectra, thereby indicating the existence of magic cluster numbers, although other cluster sizes were also detected. The occurrence of magic cluster numbers was explained by analogy to NaCl clusters, for which theoretical calculations have revealed differences in the energy for removal of one NaCl ion pair from the clusters.[8] Later theoretical studies on $[NH_4Cl]_n$ have predicted clusters with an even number of ion pairs to be more stable than those with an odd number (the only exception being n = 9) and have found an especially high stabilization for n = 4.[5]

NH_4Cl is a well known salt that crystallizes in a CsCl-type lattice. New structures emerge if one H atom is replaced by an alkyl group, hence layers of Cl^- ions are interleaved with layers of methylammonium ions in CH_3NH_3Cl.[9] The structures of some alkyldiammonium dichlorides of the general formula $[H_3N(CH_2)_nNH_3]Cl_2$ (n = 2, 5 and 7) are displayed in Figure 1.[10–12] These structures all possess infinitely extended networks where no discrete electroneutral molecular units can be found.

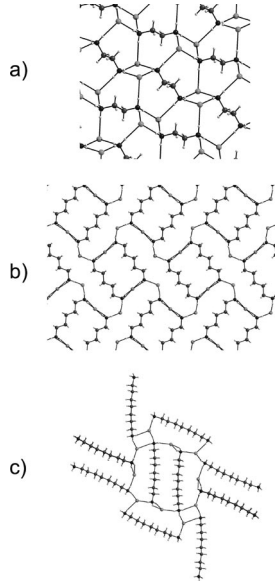

Figure 1. Sections of the crystal structures of $[H_3N(CH_2)_nNH_3]Cl_2$ compounds [n = 2 (a), 5 (b), and 7 (c)].

[a] Anorganisch-Chemisches Institut, Universität Heidelberg, Im Neuenheimer Feld 270, 69120 Heidelberg, Germany
Fax: +49-6221-545707
E-mail: hans-jorg.himmel@aci.uni-heidelberg.de
Supporting information for this article is available on the WWW under http://www.eurjic.org or from the author.

Chemists can help to understand the structures of ammonium chloride clusters by synthesizing and structurally characterizing derivatives with bulky ligands that prevent the formation of higher aggregates. This is a widely used approach for the stabilization of cluster compounds, and it will be shown herein to work also for ammonium chloride clusters.

Results and Discussion

The compound which will be discussed in the following is *N*,*N*-bis(3-amino-3,3-diallylpropyl)-4-methylbenzolsulfonamide dihydrochloride (**1**).

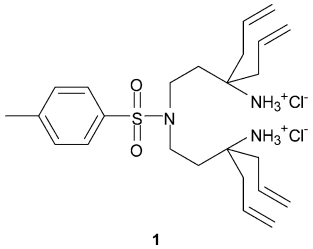

1

Its synthesis has been reported previously and requires several steps from tosylated diethanolamine.[13] This compound is a precursor to 2,2,8,8-substituted bicyclic guanidines which are used in our laboratory as ligands for group 13 (B and Ga) and group 10 (Ni and Pt) complexes.[14] Crystals suitable for X-ray diffraction were grown from ethanol. The X-ray structure analysis shows the presence of dimeric units. Figure 2 illustrates one of these units, which features a distorted cube at its center. The N and Cl atoms at alternating corners of this cube are connected through N–H···Cl hydrogen bonds. Each Cl^- anion interacts with three H atoms, and the H atoms of the next dimeric unit are more than 280 pm away from the Cl^- anions. The Cl1···N2, Cl1···N3, and Cl1···N2′ distances are 318.1(4), 317.5(2), and 312.9(2) pm, respectively, and are therefore in good agreement with the closest Cl···N separation in solid CH_3NH_3Cl [318.0(5) pm].[9]

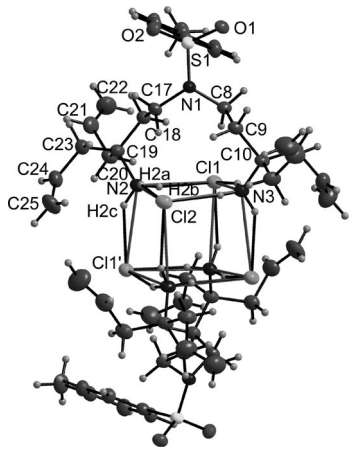

Figure 2. Crystal structure of $(\mathbf{1})_2$.

The central unit can be compared with the tetramer $[NH_4Cl]_4$ (**2**). Quantum chemical calculations using second-order Møller–Plesset perturbation theory (MP2) were carried out for this cluster and the resulting structure is illustrated in Figure 3. In good agreement with the X-ray diffraction results for derivative $(\mathbf{1})_2$, the N and Cl atoms in **2** are located at the corners of a slightly distorted cube, which leads to an overall T_d symmetry. The N···Cl separations are 309.1 pm and are thus slightly shorter than the distances found in dimeric **1** and in solid CH_3NH_3Cl.[9] The N–H bond lengths between N and the H atoms not engaged in hydrogen bonding are calculated to be 101.2 pm, while the other N–H bond lengths are significantly longer (104.2 pm). The shortest Cl···H distance is 207.1 pm.

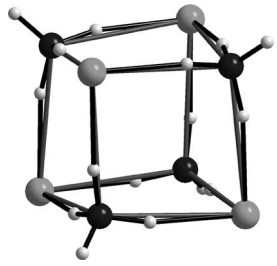

Figure 3. Calculated minimum structure of **2**.

The Raman spectrum of CH_3NH_3Cl in its α-phase (which is the stable phase at room temperature) shows the symmetric (a_1) and asymmetric NH_3^+ stretching (e) modes at 2980 and 3086 cm^{-1} and the symmetric and asymmetric NH_3 bending modes at 1556 and 1530 cm^{-1}, respectively.[15] These positions can be compared with those found and calculated for dimeric **1** and **2**. Figure 4 shows the Raman spectra of **1** in the crystalline solid state, where it contains only dimeric units, and in H_2O and MeOH solution, where it should be present as the monomer. No signal appears above 3200 cm^{-1}, which argues for a significant red-shift of the N–H stretches caused by the NH···Cl bonding. The signals at 1642/1602 cm^{-1} most likely belong to the ν(C=C)

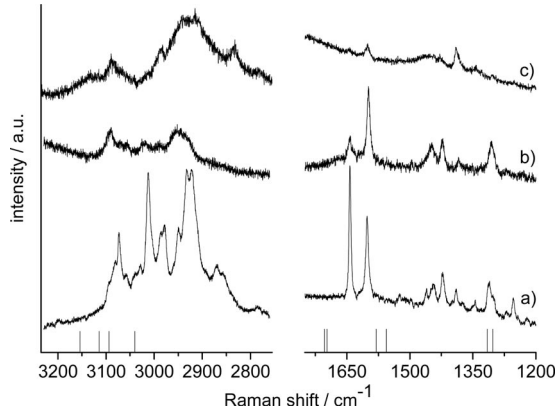

Figure 4. Raman spectra of **1** excited at 514 nm in the regions around 3000 (C–H and N–H stretching region) and 1500 cm^{-1} (NH_3 and CH_2 deformation as well as C=C stretching region) measured a) in the crystalline solid state, b) dissolved in H_2O, and c) in MeOH.

rather than $\delta(NH_3)$ modes. At least three (smaller) signals (at 1461, 1344, and 1254 cm^{-1}) in the region around 1500 cm^{-1} are visible in the spectrum of the crystalline sample but are absent from the solution spectra. These signals are therefore tentatively assigned to $\delta(NH_3)$ modes.

To obtain more information we determined vibrational wavenumbers for a $[DNH_3Cl]_4$ tetramer in which the four H atoms of **2** that are not bound to the Cl^- anions are replaced by D to minimize mode coupling by MP2 calculations. Modes at 3114 (a_1), 3040 (e), 3040 (t_1) and 3154, and 3094 cm^{-1} (t_2) can be assigned to the N–H stretching of $[DNH_3Cl]_4$, and modes at 1580 (a_1), 1703, 1303 (e), 1671, 1301 (t_1) and 1697, 1556, and 1316 cm^{-1} (t_2) belong to NH_3 bending (see Supporting Information for a complete list of wavenumbers of $[NH_4Cl]_4$ and $[DNH_3Cl]_4$). Of these, the t_1 modes are Raman- and IR-inactive. The positions of the Raman-active modes are included in Figure 4 (neglecting intensities, which were not calculated). It can be concluded that the measured spectrum of dimeric **1** gives evidence for signals in the regions where the modes of $[DNH_3Cl]_4$ are predicted to appear. A detailed analysis of the experimental spectrum is, however, difficult due to the number of different modes which fall into the two regions and would certainly require isotopic labelling experiments. These experiments are beyond the scope of this paper.

Finally, we recorded the ESI^+ spectra of **1** dissolved in MeOH and CH_2Cl_2.[16] The solubility of **1** in CH_2Cl_2 is so low that only very weak signals were detected in the Raman spectra. Nevertheless, the ESI^+ spectra show signals of sufficient intensity. Surprisingly, relatively strong features with baseline signals at *m*/*z* 999.4906 and 1516.7208, which can be assigned to the cations $[(\mathbf{1})_2 - Cl]^+$ and $[(\mathbf{1})_3 - Cl]^+$ (calculated baseline signals at *m*/*z* values of 999.4899 and 1516.7196; see Figure 5 for the isotopic pattern and a simulation), were detected. No signal assignable to a monomeric species such as $[\mathbf{1} - Cl]^+$ or $[\mathbf{1} - Cl - HCl]^+$ was visible in the spectra. The ESI^+ spectra recorded for **1** dissolved in MeOH look completely different. Thus, a group of signals with the baseline signal at *m*/*z* 446.2838, which can be assigned to the cation $[\mathbf{1} - Cl - HCl]^+$ (calculated baseline signal at *m*/*z* 446.2836), dominates the spectrum. Signals indicating the presence of trimeric units are just visible but are extremely weak (with the signals due to the trimer being even larger than those of the dimer). Thus, the ESI^+ results indicate that dimeric and even trimeric units are present in CH_2Cl_2 solutions, whereas solutions in the more polar solvent MeOH contain almost exclusively monomeric units. DFT (BP86) calculations were carried out to see if the dimeric units observed in solid **1** are stable in the gas phase and to obtain information on the likely structures of an individual molecule of **1** and of $[\mathbf{1} - 2Cl]^{2+}$. The calculated minimum structures are displayed in Figure 6, where it can be seen that the structure of the dimer resembles the structure measured in the crystalline phase. These calculations therefore predict the dimer to be stable in the gas phase. In the structure calculated for the monomer the two Cl^- anions are engaged in hydrogen bonding to both ammonium groups and the geometry is not much different from that of the dimer. As anticipated, removal of the Cl^- anions brings about a significant conformational change. The dimerization energy of **1** due to formation of N–H···Cl interactions is calculated to be 136 kJ mol^{-1}.

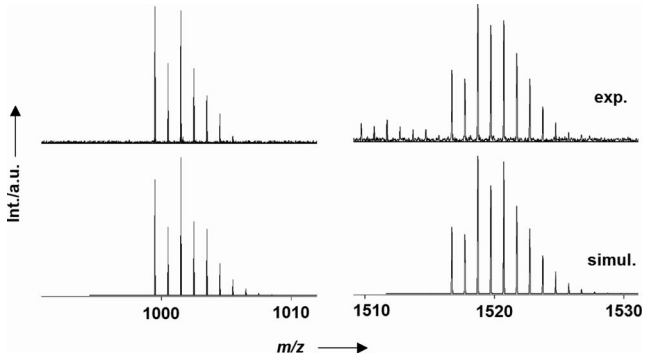

Figure 5. ESI^+ mass spectra recorded for **1** dissolved in CH_2Cl_2 in the regions around *m*/*z* 990 and 1519, and simulation of the isotopic patterns expected for $[(\mathbf{1})_2 - Cl]^+$ and $[(\mathbf{1})_3 - Cl]^+$.

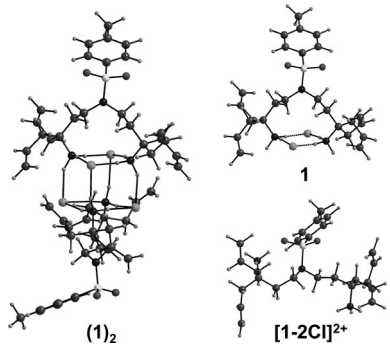

Figure 6. Calculated (BP68/SVP) structures of monomeric and dimeric **1** as well as $[\mathbf{1} - 2Cl]^{2+}$.

Conclusions

In summary, we have synthesized and structurally characterized a derivative of the tetrameric cluster $[NH_4Cl]_4$, which is one of the species that might be formed in the course of the nucleation process by which NH_4Cl is formed from HCl and NH_3 in the gas phase. Our results might help to understand this fundamental process. The ESI^+ mass spectra indicate that dimeric and trimeric units are stable in CH_2Cl_2 solution, while a methanol solution contains almost exclusively monomers.

Experimental Section

The synthesis of **1** was carried out as described in the literature.[13] ^1H NMR (400 MHz, $CDCl_3$): δ = 1.98 (m, 4 H, H1), 2.28 (m, 8 H, H2), 2.42 (s, 3 H, H3), 3.69 (m, 4 H, H4), 5.23–5.31 (dd, ^2J = 17.6, ^3J = 13.8 Hz, 8 H, H5), 5.70–5.80 (m, 4 H, H6), 7.26 (d, ^3J = 8.0 Hz, 2 H, H7), 7.63 (d, ^3J = 8.0 Hz, 2 H, H8), 8.36 (br. s, 6 H, H9) ppm. ^{13}C NMR (100 MHz, $CDCl_3$): δ = 21.5 (C3), 34.5 (C1), 39.7 (C2), 40.8 (C4), 59.2 (C10), 122.3 (C5), 126.8 (C8), 129.3

(C6), 129.8 (C7), 138.2 (C11), 143.4 ppm (C12). The assignment of the signals in the ^{13}C NMR spectrum is based on ^{1}J-CH correlation in HSQC experiments.

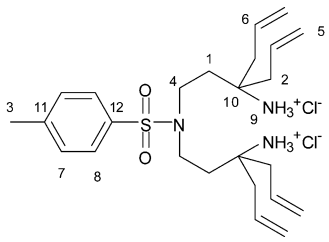

Crystals of **1** were grown from an ethanol solution. Suitable crystals were taken directly out of the mother liquor, immersed in perfluorinated polyether oil, and fixed on top of a glass capillary. Intensity data were collected on a Nonius-Kappa CCD diffractometer fitted with low-temperature unit using graphite-monochromated Mo-K_α radiation. The temperature was set to 200 K. The data collected were processed using the standard Nonius software.[17] All calculations were performed using the SHELXT-PLUS software package. Structures were solved by direct methods with the SHELXS-97 program and refined with the SHELXL-97 program.[18,19] Graphical handling of the structural data during solution and refinement was performed with XPMA.[20] Atomic coordinates and anisotropic thermal parameters of non-hydrogen atoms were refined by full-matrix least-squares calculations (Tables 1 and 2).

Table 1. Selected bond lengths [pm] and angles [°] for $(\mathbf{1})_2$ as determined by X-ray diffraction.

Cl1···N2	318.1(4)	N2···Cl2	315.1(2)
Cl2···N3	318.6(1)	N3···Cl1	317.5(2)
N2···Cl1′	312.9(1)	N2–H2a	89
N2–H2b	89	N2–H2c	89
H2a···Cl2	230.8	H2b···Cl1	229.8
H2c···Cl1′	236.2	N3–C10	151.1(3)
C10–C9	153.4(3)	C9–C8	153.4(3)
C8–N1	148.1(3)	N1–S1	163.24(19)
S1–O1	143.10(16)	S1–O2	142.85(16)
N1–C17	147.7(3)	C17–C18	153.2(3)
C18–C19	153.8(3)	C19–N2	150.3(3)
C19–C20	153.8(3)	C19–C23	154.0(3)
C20–C21	148.7(4)	C23–C24	149.7(3)
C21–C22	130.6(4)	C24–C25	131.2(4)
N2···Cl1···N3	79.20(5)	N2···Cl2···N3	79.48(5)
Cl1···N2···Cl2	100.72(6)	Cl1···N3···Cl2	100.12(6)
Cl1···N2···Cl1′	92.92(5)	N2–H2a···Cl2	158.0
N2–H2b···Cl1	172.7	N2–H2c···Cl1′	144.3

CCDC-670181 contains the supplementary crystallographic data for compound **1**. These data can be obtained free of charge from The Cambridge Crystallographic Data Center via www.ccdc.cam.ac.uk/data_request/cif.

ESI^+ mass spectra were recorded with a 9.4 T Bruker ApexQe Qh-ICR hybrid instrument (Bruker Daltonik GmbH, Bremen, Germany) with an Apollo II MTP ion source (ESI^- to MALDI switchable) in positive-ion electrospray ionization (ESI) mode. Sample solutions in methanol or dichloromethane at concentrations of 10^{-4}–10^{-5} M were admitted to the ESI interface by means of a syringe pump at 5 μL min^{-1} and sprayed at 4.5 kV (desolvation gas flow of 2.00 L min^{-1} at 220 °C, and nebulizer gas flow of 1.00 L min^{-1} for the methanolic solution). In dichloromethane, the sample was injected with a syringe pump at a rate of 10–15 μL min^{-1}, the desolvation gas flow was 1.50 L min^{-1} at 170 °C, and the nebulizer gas flow was 0.70 L min^{-1}. The mass spectra were acquired in the broadband mode with 1 million data points. Typically, about eight transients for the methanolic solution and 24 transients for the dichloromethane solution were accumulated for one magnitude spectrum. External mass calibration was performed with $[\text{arginine}_n + H]^+$ cluster ions prior to analysis to achieve a mass accuracy of 1 ppm. The instrument was controlled by Bruker ApexControl 2.0.0 software and data analysis was performed using the Bruker DataAnalysis 3.4 software.

Table 2. Crystal data and refinement details of **1**.

Formula	$C_{25}H_{41}Cl_2N_3O_2S$
M_r [g mol^{-1}]	518.57
Crystal size [mm]	0.50 × 0.30 × 0.20
Crystal system	monoclinic
Space group	*C*2/*c*
a [pm]	2779.7(6)
b [pm]	1549.5(3)
c [pm]	1342.1(3)
β [°]	98.86(3)
V [pm^3]	5.712(2)·10^9
$\rho_{calcd.}$ [g cm^{-3}]	1.206
Z	8
F(000)	2224
hkl range	–35–36, ±20, ±17
θ range [°]	1.51–27.47
μ [mm^{-1}]	0.326
T_{max}/T_{min}	0.889/0.937
Measured reflections	12847
Unique reflections (r_{int})	6530 (0.0538)
Observed reflections [$I > 2\sigma(I)$]	4182
Refined parameters/restraints	301/0
Goodness-of-fit	1.023
R_1 [$I > 2\sigma(I)$]	0.0493
*wR*2 (all data)	0.1256
Residual electron density [e Å^{-3}]	0.615/–0.320

A Horiba Jobin Yvon T64000 spectrometer was used for the Raman measurements. The Raman spectra were excited with the 514-nm line of an Ar^+ ion laser operating at 300 mW. The samples were sealed in glass tubes and measured through a microscope. IR spectra (KBr disks) were recorded with a BIORAD Excalibur FTS 3000 spectrometer and NMR spectra were measured with a Bruker Avance II 400 spectrometer.

Details of the Quantum Chemical Calculations: The MP2 calculations on **2** were carried out with the TURBOMOLE program[21] using the approximate resolution of the identity[22] to speed up the calculations. This approach decomposes the four index integrals into a sum over products of three index quantities, one index of which refers to the auxiliary basis. Hence, to transform the integrals into the molecular orbital basis the transformation has to be performed only on a smaller set of three index quantities. The def2-TZVPP basis set was used[23] along with the appropriate auxiliary TZVPP basis set for the resolution of the identity approximation.[24] Vibrational frequencies were obtained by numerical differentiation of analytically calculated gradients (NumForce tool).

DFT calculations on dimeric and monomeric **1** as well as $[\mathbf{1} - 2Cl]^{2+}$ were carried out using the BP86 functional[25] (BP is the short notation for Becke–Perdew and is a gradient-corrected DFT method employing the Becke exchange and Perdew correlation functionals) and the def2-SVP basis set.[23] Vibrational frequencies were then obtained by analytical differentiation.

Supporting Information (see also the footnote on the first page of this article): a) Calculated vibrational frequencies of $[NH_4Cl]_4$ and

$[DNH_3Cl]_4$. b) IR spectrum of solid **1** (CsI disk). c) Calculated coordinates and energies of monomeric and dimeric **1** as well as $[\mathbf{1} - 2Cl]^{2+}$.

Acknowledgments

We are grateful to Dr. Gross for performing the ESI^+ measurements and to the Deutsche Forschungsgemeinschaft (DFG) and the Fonds der Chemischen Industrie for financial support.

[1] a) A. Laaksonen, V. Talanquer, D. W. Oxtoby, *Annu. Rev. Phys. Chem.* **1995**, *46*, 489–524; b) D. W. Oxtoby, *Acc. Chem. Res.* **1998**, *31*, 91–97.
[2] J. Heintzenberg, *Tellus, Ser. B* **1989**, *41*, 149–160.
[3] V.-M. Kerminen, A. S. Wexler, S. Potukuchi, *J. Geophys. Res.* **1997**, *102*, 3715–3724, and references cited therein.
[4] F.-M. Tao, *J. Chem. Phys.* **1999**, *110*, 11121–11124, and references cited therein.
[5] A. Matro, D. L. Freeman, R. Q. Topper, *J. Chem. Phys.* **1996**, *104*, 8690–8702.
[6] G. Schmelzeisen-Redeker, S. S. Wong, U. Giessmann, F. W. Röllgen, *Z. Naturforsch., Teil A* **1985**, *40*, 430–431.
[7] H. Nehring, S. Thiebes, L. Bütfering, F. W. Röllgen, *Int. J. Mass Spectrom. Ion Processes* **1993**, *128*, 123–132.
[8] T. P. Martin, *J. Chem. Phys.* **1978**, *69*, 2036–2042.
[9] E. W. Hughes, W. N. Lipscomb, *J. Am. Chem. Soc.* **1946**, *68*, 1970–1975.
[10] a) H. Reuter, G. Kastner, *Z. Kristallogr.-New. Cryst. Struct.* **1997**, *212*, 188; b) M. Bujak, L. Sikorska, J. Zaleski, *Z. Anorg. Allg. Chem.* **2000**, *626*, 2535–2542.
[11] I. Pospieszna-Markiewicz, W. Radecka-Paryzek, M. Kubicki, *Acta Crystallogr., Sect. C: Cryst. Struct. Commun.* **2006**, *62*, o399–o401.
[12] J. Brisson, A. L. Beauchamp, *Acta Crystallogr., Sect. C: Cryst. Struct. Commun.* **1988**, *44*, 1152–1153.
[13] F. P. Schmidtchen, *Chem. Ber.* **1980**, *113*, 2175–2182.
[14] See, for example, for group 13: a) G. Robinson, C. Y. Tang, R. Köppe, A. R. Cowley, H.-J. Himmel, *Chem. Eur. J.* **2007**, *13*, 2648–2654; b) O. Ciobanu, P. Roquette, S. Leingang, H. Wadepohl, J. Mautz, H.-J. Himmel, *Eur. J. Inorg. Chem.* **2007**, 4530–4534; c) R. Dinda, O. Ciobanu, H. Wadepohl, O. Hübner, R. Acharraya, H.-J. Himmel, *Angew. Chem.* **2007**, *119*, 9270–9273; *Angew. Chem. Int. Ed.* **2007**, *46*, 9110–9113. For group 10: d) U. Wild, P. Roquette, E. Kaifer, J. Mautz, O. Hübner, H. Wadepohl, H.-J. Himmel, *Eur. J. Inorg. Chem.* **2008**, 1248–1257.
[15] N. Meinander, S. Forss, G. Bergström, *J. Raman Spectrosc.* **1981**, *11*, 155–167.
[16] The Raman spectrum of a CH_2Cl_2 solution of **1** shows virtually no signals because of poor solubility.
[17] DENZO-SMN, Data processing software, Nonius **1998**; http://www.nonius.com.
[18] a) G. M. Sheldrick, *SHELXS-97*, *Program for Crystal Structure Solution*, University of Göttingen, **1997**; http://shelx.uni-ac.gwdg.de/SHELX/index.html; b) G. M. Sheldrick, *SHELXL-97*, *Program for Crystal Structure Refinement*, University of Göttingen, **1997**; http://shelx.uni-ac.gwdg.de/SHELX/index.html.
[19] *International Tables for X-ray Crystallography*, vol. 4, Kynoch Press, Birmingham, U. K., **1974**.
[20] L. Zsolnai, G. Huttner, *XPMA*, University of Heidelberg, **1994**; http://www.uni-heidelberg.de/institute/fak12/AC/huttner/software/software.html.
[21] R. Ahlrichs, M. Bär, M. Häser, H. Horn, C. Kölmel, *Chem. Phys. Lett.* **1989**, *162*, 165–169.
[22] F. Weigend, M. Häser, *Theor. Chem. Acc.* **1997**, *97*, 331–340.
[23] F. Weigend, R. Ahlrichs, *Phys. Chem. Chem. Phys.* **2005**, *7*, 3297–3305.
[24] F. Weigend, M. Häser, H. Patzelt, R. Ahlrichs, *Chem. Phys. Lett.* **1998**, *294*, 143–152.
[25] a) A. D. Becke, *Phys. Rev. A* **1988**, *38*, 3098–3100; b) J. P. Perdew, *Phys. Rev. B* **1986**, *33*, 8822–8824.

Received: December 7, 2007
Published Online: March 28, 2008

